



A two-photon excited luminescence of water-soluble rhodamine–platinum(II) complex: Fluorescent probe specific for Hg²⁺ detection in live cell

Jun Feng Zhang^{a,b,1}, Chang Su Lim^{a,1}, Bong Rae Cho^{a,*}, Jong Seung Kim^{a,*}

^a Department of Chemistry, Korea University, Seoul 136-701, Republic of Korea

^b College of Chemistry and Chemical Engineering, Yunnan Normal University, Kunming, 650092, PR China

ARTICLE INFO

Article history:

Received 9 August 2010

Received in revised form 7 October 2010

Accepted 8 October 2010

Available online 16 October 2010

Key words:

Rhodamine

Platinum(II) complex

Hg²⁺ sensor

Two-photon microscopy

ABSTRACT

The first example of cyclometalated platinum(II)-containing rhodamine probe (**1**) with two-photon induced luminescent properties was synthesized and investigated for mercury detection. A highly selective color change of **1**, from light yellow to pink, is observed only in the presence of Hg²⁺ due to the formation of 1,3,4-oxadiazole ring in **2**. This selectivity of Hg²⁺ with color changes can be observed easily by the naked-eye. Meanwhile, a remarkable turn-on and selective 20-fold fluorescent enhancement of **1** upon binding with Hg²⁺ over the other tested metal ions was observed. The water-soluble probe **1** was successfully applied in the visualizing of the site of Hg²⁺ accumulation as well as estimating of trace amounts of mercury ions in live HeLa cells by two-photon microscopy.

© 2010 Elsevier B.V. All rights reserved.

1. Introduction

In recent years, optical imaging with two-photon microscopy (TPM) has become an important tool applied in the biological field [1–7]. Excitation with two near-infrared (NIR) photons have several advantages: (i) increased penetration depth (>500 nm) (ii) lower tissue autofluorescence and self-absorption (iii) reduced photo-damage and photobleaching, which ensure the long term imaging [3,4]. Consequently, there has been increasing interest in the development of two-photon probes that can detect biological event inside the live cell and tissue without photo damage.

Mercury is a highly poisonous element, which damages DNA, impairs mitosis, and disrupts the central nervous and endocrine systems [8,9]. In this regard, many fluorescent probes for mercury ions have been extensively explored [10–18]. Compared to traditional one-photon sensing, two-photon excited fluorescence (TPEF) microscopy using two near-infrared photons for excitation offers many advantages in the biology community [19].

Recently, platinum(II) complexes system received considerable attention in the property of nonlinear absorption and two-photon induced luminescence [20–23]. Although some cyclometalated platinum(II) complex showing two-photon imaging in live cells have been reported for the potential advantages including the long

resident lifetime in biology system, the high two-photon induced luminescent intensity and the low cytotoxicity [24–26], the use of organic-metal platinum(II) complex in the field of TP probes studies has been largely neglected.

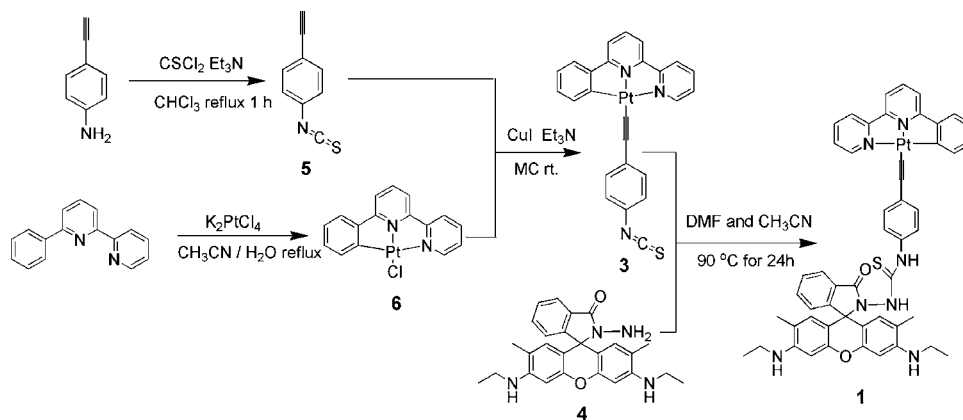
In the design of the target molecule, the well-known spiro-lactam ring-opening process of Rhodamine derivatives was introduced to ensure a turn-on fluorescence increase with an obvious color change from colorless to pink, thus enabling detection simply with the naked eye. The CNN-Pt(II)-alkynyl moiety will increase the nonlinear absorption property of this system, which is expected to be helpful to estimate trace amounts of mercury ions in live cells by two-photon microscopy. Even though various rhodamine derivatives have been reported as fluorescent chemosensors or chemodosimeters [10–18], studies on the organic-metal rhodamine system are scarce [11]. And no TP probe studies for this class of compounds have been explored.

In this study, we report a new water-soluble CNN-Pt(II)-alkynyl complex-containing rhodamine probe (**1**) for Hg²⁺ detection using the typically mercury-promoted desulfurization reaction and spiro-lactam ring opening approach (Scheme 1) [14–18]. Among the various metal ions, the chemosensor **1** displayed highly selective color changes and fluorescent increase upon the addition of Hg²⁺. As expected, CNN-Pt(II)-alkynyl moiety served successfully as a source of the two-photon absorption. As far as we are aware of, **1** is the first Hg²⁺ sensor based on CNN-Pt(II)-alkynyl complex-containing rhodamine derivative that can detect Hg²⁺ in live cells by TPM.

* Corresponding authors. Tel.: +82 232903143; fax: +82 232903121.

E-mail addresses: chobr@korea.ac.kr (B.R. Cho), jongskim@korea.ac.kr (J.S. Kim).

¹ Equally contributed to this work.



Scheme 1. The synthesis route of compound **1**.

2. Experimental

2.1. Apparatus

NMR was recorded at OXFORD NMR (300 MHz, Oxford Instrument, UK) and mass spectra were recorded at Matrix-assisted laser desorption ionization mass spectrometer (MALDI-TOF, Applied Biosystems Inc., USA). UV–vis absorption spectra were recorded in S-3100 spectrophotometer (Scinco, Seoul, Korea). Fluorescence spectra were recorded in RF-5301PC spectrophotometer (Shimadzu Scientific Instruments Inc. Tokyo, Japan). Two-photon fluorescence microscopy images of **1**-labeled cells and tissues were obtained with spectral confocal and multiphoton microscopes (Leica TCS SP2) with a $\times 100$ (NA = 1.30 OIL) objective lens, respectively.

2.2. Materials

All reagents and solvents for synthesis were commercial and used without further purification. All the reactions have been performed under high pure nitrogen or argon atmosphere. Synthesized products have been purified by column chromatography on silica gel (100–200 mesh). Compounds 6-phenyl-2,2'-bipyridine, CNN-Pt-Cl (**6**) and Rodamine 6G hydrazide (**4**) were synthesized by an improved method according to the literature [27,14]. Synthesis of other compounds is described below (Scheme 1).

2.3. Synthesis of compound **1**

Compound **5**: 4-Ethynylbenzenamine (2.0 g, 17.1 mmol) and triethylamine (10 ml, 71.6 mmol) in 30 ml CHCl_3 were placed in a flask under an atmosphere of N_2 . A solution of thiophosgene (3 mL, 38.6 mmol) in 20 ml CHCl_3 was added dropwise at room temperature for 1 h. The mixture was heated under reflux for 2 h, and then cooled to room temperature. The above mixture was quenched by addition of 20 mL cool water and extracted with 300 mL (3×100 mL) CHCl_3 . The organic layers were washed with H_2O (3×50 mL), dried (Na_2SO_4) and concentrated to dryness to give a yellow residue. This was purified by chromatography on silica gel using a hexane/dichloromethane mixture (5:1) as eluent. A pale yellow solid (**5**) was then obtained. Yield: 2.1 g (77%). ^1H NMR (CDCl_3 , 300 MHz) δ (ppm): 3.16 (s, 1H), 7.17 (d, 2H, $J = 8.7$ Hz), 7.46 (d, 2H, $J = 8.7$ Hz).

Compound **3**: CNN-Pt-Cl (**2**) (460 mg, 1 mmol), 1-ethynyl-4-isothiocyanatobenzene (**5**) (480 mg, 3 mmol), Et_3N (10 mL) and CuI (25 mg) in degassed CH_2Cl_2 was stirred under a nitrogen atmosphere at room temperature overnight. The reaction mixture was then evaporated to dryness under reduced pressure. The crude

product was purified by chromatography on silica gel using a hexane/dichloromethane mixture (2:1) as eluent. A dark red crystal (**3**) was then obtained by further purified by recrystallization from dichloromethane/diethyl ether. Yield: 430 mg (74%). ^1H NMR (d^6 -DMSO, 300 MHz) δ (ppm): 7.06 (t, 1H, $J = 7.3$ Hz), 7.12 (t, 1H, $J = 7.3$ Hz), 7.35 (d, 2H, $J = 8.6$ Hz), 7.42 (d, 2H, $J = 8.6$ Hz), 7.64 (d, 1H, $J = 7.3$ Hz), 7.71 (d, 1H, $J = 7.3$ Hz), 7.85 (t, 1H, $J = 6.0$ Hz), 8.01 (d, 1H, $J = 7.9$ Hz), 8.13 (t, 1H, $J = 7.9$ Hz), 8.23 (d, 1H, $J = 7.9$ Hz), 8.34 (t, 1H, $J = 8.0$ Hz), 8.51 (d, 1H, $J = 8.0$ Hz), 9.02 (d, 1H, $J = 6.0$ Hz). MS (FAB): $m/z = 585.1$ [$\text{M} + \text{H}$] $^+$, calc. for $\text{C}_{25}\text{H}_{15}\text{N}_3\text{PtS} = 584.06$.

Compound **1**: Et_3N (1 mL) was added to a solution of Rodamine 6G hydrazide (**4**) (86 mg, 0.20 mmol) and CNN-Pt \equiv Ph-NCS (**3**) (116 mg, 0.20 mmol) in 20 mL DMF/ CH_3CN ($v/v = 1/1$). The reaction mixture was stirred at 90 °C for 24 h. After the solvent was evaporated under reduced pressure, 20 ml water was added and extracted with 120 mL (3×40 ml) CHCl_3 . The organic layers were washed with H_2O (3×20 mL), dried (Na_2SO_4) and concentrated to dryness to give a red residue. This was purified by chromatography on silica gel using a dichloromethane/ EtOAc mixture (5:1) as eluent. A purple solid (**1**) was then obtained. Yield: 30 mg (15%). The structure of **1** was confirmed by ^1H NMR, ^{13}C NMR, and MS analysis. ^1H NMR (CDCl_3 , 300 MHz) δ (ppm): 1.33 (t, 6H, $J = 7.1$ Hz); 1.86 (s, 6H), 3.18–3.23 (m, 4H), 3.58 (broad, 2H), 6.26 (s, 2H), 6.40 (s, 2H), 6.88 (s, 1H), 6.94 (d, 2H, $J = 8.5$ Hz), 6.98–7.03 (m, 1H), 7.08–7.14 (m, 1H), 7.24 (s, 1H), 7.32 (d, 2H, $J = 8.5$ Hz), 7.40 (t, 2H, $J = 6.0$ Hz), 7.48 (d, 1H, $J = 7.7$ Hz), 7.54 (s, 1H), 7.60–7.69 (m, 3H), 7.75–7.88 (m, 4H), 8.06 (d, 1H, $J = 6.7$ Hz), 8.95 (d, 1H, $J = 5.3$ Hz). ^{13}C NMR (75 MHz, d^6 -DMSO) δ (ppm): 14.7, 17.5, 37.9, 95.9, 104.3, 105.4, 118.6, 119.7, 119.8, 123.4, 124.1, 124.6, 125.5, 125.9, 128.9, 129.1, 129.5, 130.8, 131.0, 131.1, 134.1, 136.1, 138.1, 140.6, 142.9, 147.6, 148.1, 148.2, 151.3, 151.9, 152.1, 154.8, 158.0, 164.6. MS (FAB): $m/z = 1013.31$ [$\text{M} + \text{H}$] $^+$, calc. for $\text{C}_{51}\text{H}_{43}\text{N}_7\text{O}_2\text{PtS} = 1012.2847$; $m/z = 1438.36$ [$\text{M} + \text{CNN-Pt}$] $^+$, calc. for $\text{C}_{67}\text{H}_{54}\text{N}_9\text{O}_2\text{Pt}_2\text{S} = 1438.34$.

2.4. Measurement of two-photon cross section

The two-photon cross section (δ) was determined by using femto second (fs) fluorescence measurement technique as described [28]. Upon addition of Hg^{2+} to **1** dissolved in 20 mM HEPES buffer (pH 7.0) at concentrations of 5.0×10^{-6} M and then the two-photon induced fluorescence intensity was measured at 740–940 nm by using fluorescein (8.0×10^{-5} M, pH 11) as the reference, whose two-photon property has been well characterized in the literature [29]. The intensities of the two-photon induced fluorescence spectra of the reference and sample emitted at the same excitation wavelength were determined. The two photon absorption (TPA) cross section was calculated by using $\delta = \delta_r (S_r \Phi_r \phi_r c_r) / (S_s \Phi_s \phi_s c_s)$: where the subscripts s and r stand for

the sample and reference molecules. The intensity of the signal collected by a CCD detector was denoted as S . Φ is the fluorescence quantum yield. ϕ is the overall fluorescence collection efficiency of the experimental apparatus. The number density of the molecules in solution was denoted as c . δ_r is the TPA cross section of the reference molecule.

2.5. Cell culture and imaging

HeLa human cervical carcinoma cells (ATCC, Manassas, VA, USA) were cultured in DMEM (WelGene Inc, Seoul, Korea) supplemented with 10% FBS (WelGene), penicillin (100 units/ml), and streptomycin (100 $\mu\text{g/ml}$). All the cells were maintained in a humidified atmosphere of 5/95 (v/v) of CO_2/air at 37°C . Two days before imaging, the cells were passed and plated on glass-bottomed dishes (MatTek). For labeling, the growth medium was removed and replaced with DMEM without FBS. The cells were incubated with $2\ \mu\text{M}$ **1** for 20 min at 37°C and were washed three times with DMEM without FBS. Then $20\ \mu\text{M}$ HgCl_2 was added to the cells and imaged.

2.6. Two-photon fluorescence microscopy

Two-photon fluorescence microscopy images of probe-labeled cells were obtained with spectral confocal and multiphoton microscopes (Leica TCS SP2) with a 100 (NA=1.30 OIL) objective lens. The two-photon fluorescence microscopy images were obtained with a DM IRE2 Microscope (Leica) by exciting the probes with a mode-locked titanium-sapphire laser source (Coherent Chameleon, 90 MHz, 200 fs) set at wavelength 780 nm and output power 1230 mW, which corresponded to approximately 10 mW average power in the focal plane. To obtain images at 480–640 nm range, internal PMTs were used to collect the signals in an 8 bit unsigned 1024×1024 pixels at 400 Hz scan speed.

3. Results and discussion

3.1. UV–vis titration studies

The absorption spectrum of **1** shows the typical $\text{Pt}(\text{CNN})\text{C}\equiv\text{C}-\text{C}_6\text{H}_4$ moiety absorption bands in the region of 250–380 nm which was responsible for its pale yellow color, indicating that the rhodamine part exists as the spirolactam form. Upon addition of increasing amounts of Hg^{2+} ions to a solution of **1** (1×10^{-5} M) in spectroscopic grade CH_3CN and HEPES buffer (20 mM, pH 7.0, v/v 50/50), a new absorption band centered at 535 nm appeared with increasing intensity and reached its maximum upon addition of 1 equivalent Hg^{2+} ions, which induced a clear color change from pale yellow to pink (Fig. 1).

3.2. Fluorescent studies

To further explore the utility of **1** as an ion-selective fluorescence sensor for Hg^{2+} ion, the fluorogenic behavior of **1** was investigated under the same conditions. Upon addition of the Hg^{2+} ions, a significant increase of the fluorescence intensity (with 23-fold) at 545 nm was observed (Fig. 2). The fluorescence intensity of **1** solution was linearly proportional to the amount of Hg^{2+} added in μM level with detection limit of 4.87×10^{-7} M in CH_3CN and HEPES buffer. By plotting the changes in **1** in the emission intensity at 545 nm as a function of Hg^{2+} concentration, a sigmoidal curve were obtained and is shown in the inset of Fig. 2. To corroborate 1:1 ratio between **1** and Hg^{2+} , Job's plot analyses were also executed and confirmed the 1:1 stoichiometry (Fig. S1). Both UV–vis and fluorescence data showed significant OFF–ON signals, which showed that the addition of the Hg^{2+} ion could induce desulfurization reaction (Scheme 2), and spirolactam ring opening of the spirolactam of

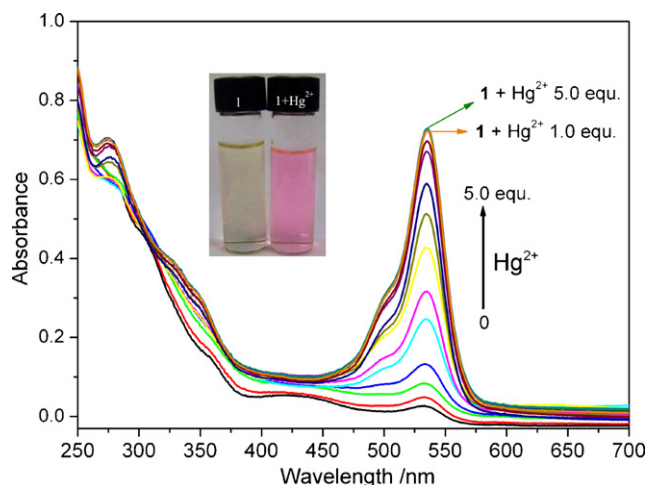


Fig. 1. The UV absorption changes of **1** ($10\ \mu\text{M}$) upon additions of Hg^{2+} in $\text{CH}_3\text{CN}/\text{HEPES}$ buffer (20 mM, pH 7.0, v/v 50/50). Inset: Color changes of **1** ($10\ \mu\text{M}$) upon additions of Hg^{2+} ($10\ \mu\text{M}$) in CH_3CN and HEPES buffer (20 mM, pH 7.0, v/v 50/50).

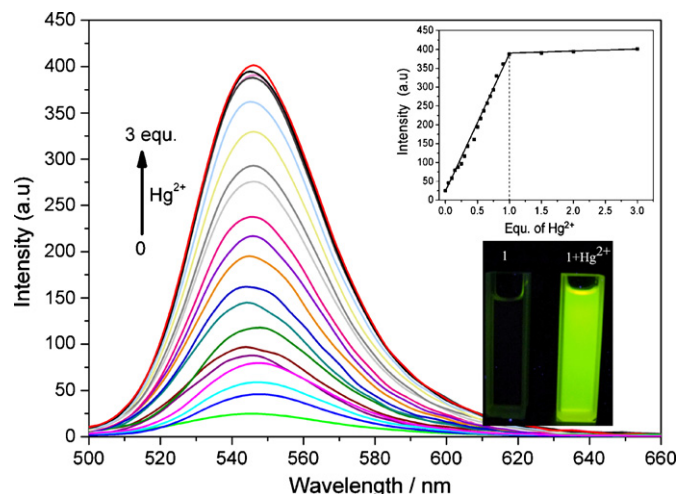
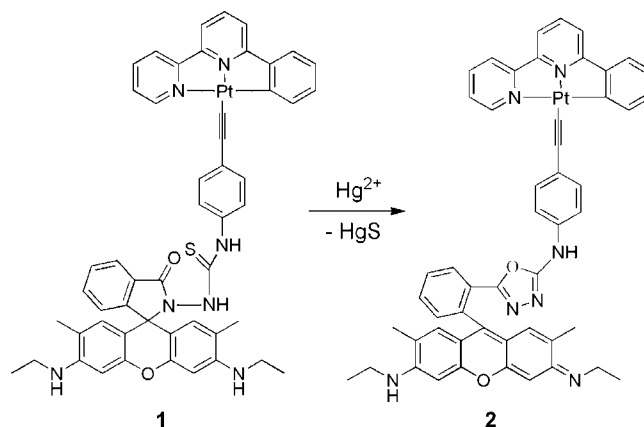


Fig. 2. Fluorescence spectra (excitation at 490 nm) of **1** ($2\ \mu\text{M}$) in $\text{CH}_3\text{CN}/\text{HEPES}$ buffer (20 mM, pH 7.0, v/v 50/50) in the presence of Hg^{2+} . Inset: Fluorescence intensity changes (at 545 nm) vs equivalents of Hg^{2+} (up); Fluorescence images of **1** ($10\ \mu\text{M}$) before and after additions of Hg^{2+} ($10\ \mu\text{M}$) in $\text{CH}_3\text{CN}/\text{HEPES}$ buffer (20 mM, pH 7.0, v/v 50/50) excited at 365 nm (down).



Scheme 2. Hg^{2+} -promoted desulfurization and ring opening of **1**.

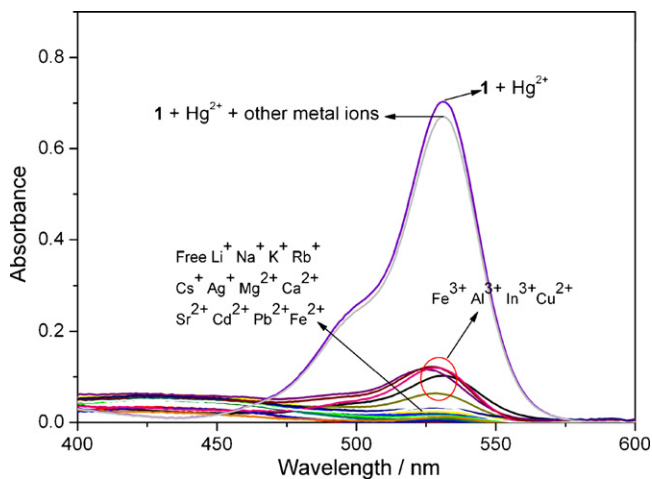


Fig. 3. The UV absorption spectra of **1** (10 μM) in CH_3CN and HEPES buffer (20 mM, pH 7.0, v/v 50/50) upon addition of various metal cation perchlorates (each concentration was 50 μM).

rhodamine could take place rapidly at room temperature. The formation of **2** has been confirmed by the $m/z = 980.34$ peak observed in ESI MS analysis (Fig. S6).

3.3. Interference from other metal ions

Beside the high sensitivity, another important feature of **1** is its high selectivity toward Hg^{2+} over other competitive species. The absorption and fluorescence properties of **1** towards other metal ions, including Li^+ , Na^+ (100 equiv.), K^+ (100 equiv.), Rb^+ , Cs^+ , Ag^+ , Mg^{2+} , Ca^{2+} , Sr^{2+} , Cd^{2+} , Pb^{2+} , Fe^{2+} , Cu^{2+} , Zn^{2+} , Fe^{3+} , Al^{3+} , and In^{3+} were also measured (Figs. 3 and 4). The miscellaneous competitive cations did not lead to significant absorption in the visible region and fluorescence changes. Moreover, in the presence of miscellaneous competitive cations, the Hg^{2+} ion still lead to the similar absorption and fluorescence changes. In addition, the increases of absorbance and fluorescence intensity resulting from the addition of the Hg^{2+} ion were not influenced by the subsequent addition of miscellaneous cations. These results implied that the selectivity of **1** toward Hg^{2+} was remarkable and made **1** as a selective chromogenic and fluorescent sensor for Hg^{2+} ions.

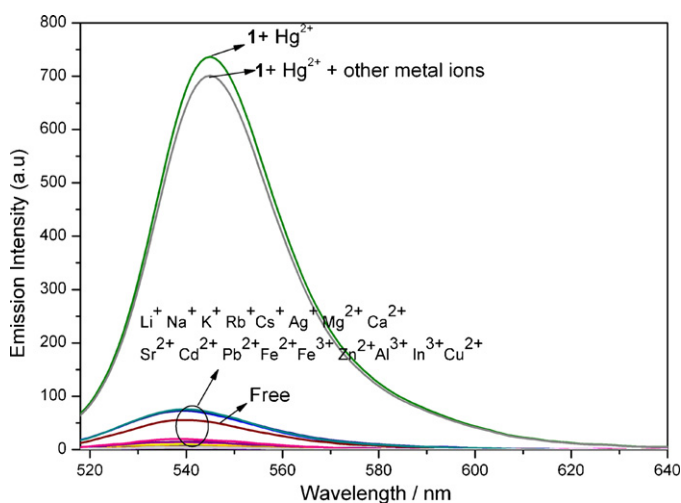


Fig. 4. Fluorescence spectra of **1** (10 μM) in CH_3CN and HEPES buffer (20 mM, pH 7.0, v/v 50/50) upon addition of various metal cation perchlorates (each concentration was 50 μM) with an excitation wavelength of 490 nm.

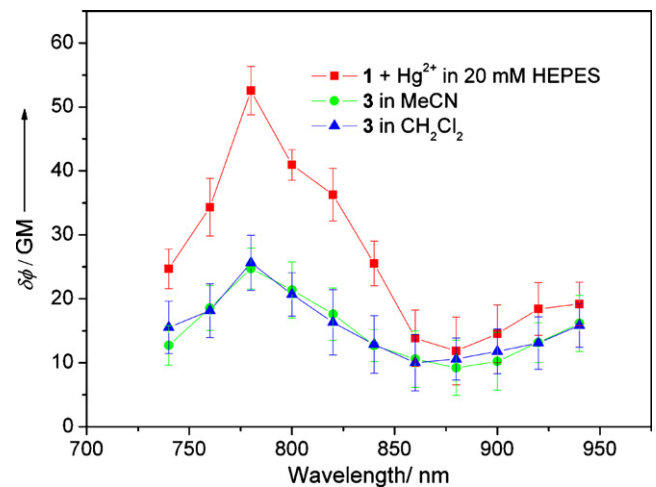


Fig. 5. Two-photon action spectrum of **1** (2.0 μM) in the presence of 2 μM Hg^{2+} (20 mM HEPES, pH 7.2) and **3** (10 μM) in each acetonitrile and dichloromethane. Error bars from replicate experiments ($n = 5$).

3.4. Two-photon excitation spectra

Fig. 5 shows the TP excitation spectra of **3** (10 μM) in acetonitrile and dichloromethane and of **1** (2.0 μM) in the presence of Hg^{2+} (2 μM) in the HEPES buffer. The TPA cross section of **3** was 25 GM at 780 nm in both acetonitrile and dichloromethane, which is larger than those of the recently reported cyclplatinated complexes (~ 20 GM, 1×10^{-3} M in DMF) as well as the previous reported platinum(II) acetylide complexes (5–10 GM) [24,30]. Moreover, TPA cross section of **1** after addition of Hg^{2+} in the HEPES was 55 GM at 780 nm. Further, the TP fluorescence intensity of **1** in HEPES buffer increased by ~ 20 -fold after addition of Hg^{2+} ions (Fig. 6). The results point out that **1** could be useful as a TP probe for Hg^{2+} in aqueous medium.

3.5. Two-photon cell imaging

The TP excited fluorescence (TPEF) intensity at a given position on the **1**-labeled HeLa cells treated with Hg^{2+} and maintained nearly the same after continuous irradiation of the fs-pulses for 2000 s, indicating its high photostability (Fig. S2). To confirm the utility of this probe, we tested the capability of **1** to detect the Hg^{2+} in live cells (Fig. 7). The TPM image of HeLa cells labeled with **1** (2 μM) for 20 min at 37 $^\circ\text{C}$ showed weak fluorescence (Fig. 7a), presumably due to the efficient fluorescence quenching by photoinduced elec-

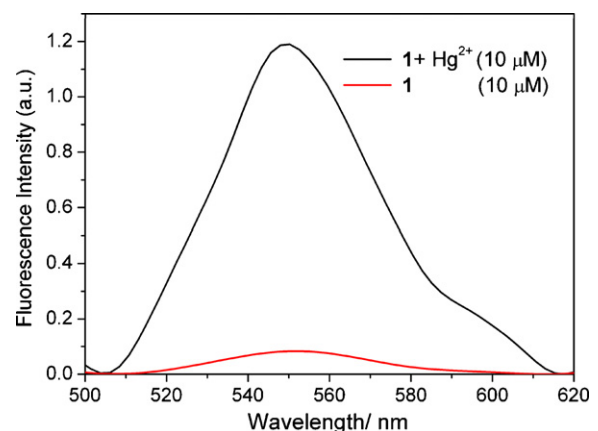


Fig. 6. Two-photon emission spectra of **1** in the presence of 10 μM Hg^{2+} (20 mM HEPES, pH 7.0, v/v 50/50) with an excitation wavelength of 780 nm.

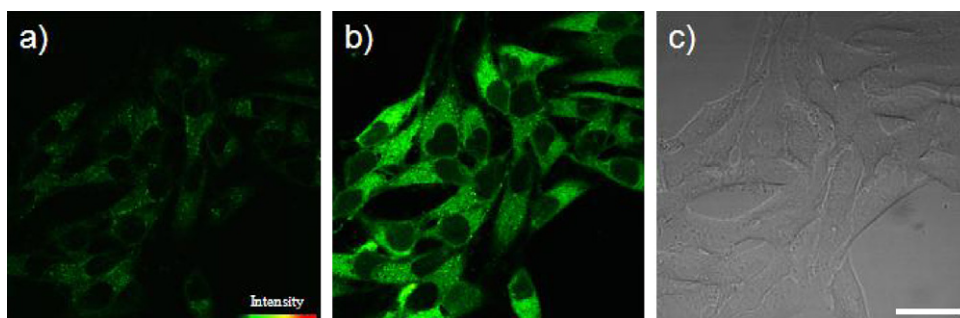


Fig. 7. (a–c) TPM image of HeLa cells labeled with **1** (2 μM) before (a) and after (b) addition of Hg^{2+} (20 μM) for 30 min. (c) Bright-field image of cells. The TPEF was collected at 480–640 nm upon excitation at 780 nm with fs pulse. Scale bars, 30 μm .

tron transfer (PET) [31,32]. The TPEF increased significantly when the cells were treated with 20 μM of Hg^{2+} for 30 min (Fig. 4b). The TPEF increased sensitively according to gradual addition of Hg^{2+} for 30 min (Fig. S10). The bright field image shows that the cells remain intact during the imaging (Fig. 4c). Hence, **1** is highly useful TPEF sensor for detecting Hg^{2+} in live cells.

4. Conclusions

A new cyclometalated platinum(II)-rhodamine derivative has been synthesized as a turn-on fluorescence probe for the detection of Hg^{2+} in aqueous solution. This is the first organic cyclometalated platinum(II)-containing rhodamine sensor with excitation in the visible region and 20-fold turn-on fluorescence emission and features excellent selectivity for Hg^{2+} over other metal ions. Moreover, two-photon microscopy experiments indicate that **1** can be used for bioimaging of Hg^{2+} . Furthermore, cyclometalated platinum(II) moiety successfully increased the TP absorption properties of **1**. We anticipate that this probe will be of great benefit to biomedical researchers for studying the effects of Hg^{2+} in biological systems.

Acknowledgements

This work was supported by the CRI project (2010-0000728) (J.S. Kim), NRF grant (ROA-2010-0018921), and Priority Research Centers Program through the NRF funded by the Ministry of Education, Science and Technology (No. 2010-0020209) (B.R. Cho). J.F. Zhang acknowledges the “ChunHui Project” Foundation of ministry of education of China, the Foundation of Department of Education of Yunnan Province of China (08Y0137) and the Foundation of Department of Science and Technology of Yunnan Province of China (2008CD104). CSL was supported by a BK21 scholarship.

Appendix A. Supplementary data

Supplementary data associated with this article can be found, in the online version, at doi:10.1016/j.talanta.2010.10.016.

References

- [1] W.R. Zipfel, R.M. Williams, W.W. Webb, *Nat. Biotechnol.* 21 (2003) 1369–1377.
- [2] F. Helmchen, W. Denk, *Nat. Methods* 2 (2005) 932–940.
- [3] H.M. Kim, B.R. Cho, *Acc. Chem. Res.* 42 (2009) 863–872.
- [4] Y.S. Tian, H.Y. Lee, C.S. Lim, J. Park, H.M. Kim, Y.N. Shin, E.S. Kim, H.J. Jeon, S.B. Park, B.R. Cho, *Angew. Chem., Int. Ed.* 48 (2009) 8027–8031.
- [5] H.M. Kim, M.S. Seo, M.J. An, J.H. Hong, Y.S. Tian, J.H. Choi, O. Kwon, K.J. Lee, B.R. Cho, *Angew. Chem., Int. Ed.* 47 (2008) 5167–5170.
- [6] H.M. Kim, B.H. Jeong, J.Y. Hyon, M.J. An, M.S. Seo, J.H. Hong, K.J. Lee, C.H. Kim, T. Joo, S.C. Hong, B.R. Cho, *J. Am. Chem. Soc.* 130 (2008) 4246–4247.
- [7] J.H. Lee, C.S. Lim, Y.S. Tian, J.H. Han, B.R. Cho, *J. Am. Chem. Soc.* 132 (2010) 1216–1217.
- [8] E.M. Nolan, S.J. Lippard, *Chem. Rev.* 108 (2008) 3443–3480.
- [9] J.C. Clifton, *Pediatr. Clin. N. Am.* 54 (2007) 237–269.
- [10] M.H. Lee, J.S. Wu, J.W. Lee, J.H. Jung, J.S. Kim, *Org. Lett.* 9 (2007) 2501–2504.
- [11] H. Yang, Z. Zhou, K. Huang, M. Yu, F. Li, T. Yi, C. Huang, *Org. Lett.* 9 (2007) 4729–4732.
- [12] X. Chen, S.W. Nam, M.J. Jou, Y. Kim, S.J. Kim, S. Park, J. Yoon, *Org. Lett.* 10 (2008) 5235–5238.
- [13] J. Huang, Y. Xu, X. Qian, *J. Org. Chem.* 74 (2009) 2167–2170.
- [14] Y.K. Yang, K.J. Yook, J. Tae, *J. Am. Chem. Soc.* 127 (2005) 16760–16761.
- [15] S.K. Ko, Y.K. Yang, J. Tae, I. Shin, *J. Am. Chem. Soc.* 128 (2006) 14150–14155.
- [16] J.S. Wu, I.C. Hwang, K.S. Kim, J.S. Kim, *Org. Lett.* 9 (2007) 907–910.
- [17] X. Zhang, Y. Xiao, X. Qian, *Angew. Chem. Int. Ed.* 47 (2008) 8025–8029.
- [18] M.H. Lee, S.W. Lee, S.H. Kim, C. Kang, J.S. Kim, *Org. Lett.* 11 (2009) 2101–2104.
- [19] S.L. Chang, D.W. Kang, Y.S. Tian, J.H. Han, H.L. Hwang, B.R. Cho, *Chem. Commun.* 46 (2010) 2388–2390.
- [20] Z.D. Yang, J.K. Feng, A.M. Ren, *Inorg. Chem.* 47 (2008) 10841–10850.
- [21] P. Shao, Y. Li, J. Yi, T.M. Pritchett, W. Sun, *Inorg. Chem.* 49 (2010) 4507–4517.
- [22] D.C. Flynn, G. Ramakrishna, H.B. Yang, B.H. Northrop, P.J. Stang, T. Goodson, *J. Am. Chem. Soc.* 132 (2010) 1348–1358.
- [23] C.H. Tao, H. Yang, N. Zhu, V.W.W. Yam, S.J. Xu, *Organometallics* 27 (2008) 5453–5458.
- [24] C.K. Koo, K.L. Wong, C.W.Y. Man, Y.W. Lam, L.K.Y. So, H.L. Tam, S.W. Tsao, K.W. Cheah, K.C. Lau, Y.Y. Yang, J.C. Chen, M.H.W. Lam, *Inorg. Chem.* 48 (2009) 872–878.
- [25] C.K. Koo, K.L. Wong, C.W.Y. Man, H.L. Tam, S.W. Tsao, K.W. Cheah, M.H.W. Lam, *Inorg. Chem.* 48 (2009) 7501–7503.
- [26] C.K. Koo, L.K.Y. So, K.L. Wong, Y.M. Ho, Y.W. Lam, M.H.W. Lam, K.W. Cheah, C.C.W. Cheng, W.M. Kwok, *Chem. Eur. J.* 16 (2010) 3942–3950.
- [27] J.H.K. Yip, Suwarno, J.J. Vittal, *Inorg. Chem.* 39 (2000) 3537–3543.
- [28] S.K. Lee, W.J. Yang, J.J. Choi, C.H. Kim, S.J. Jeon, B.R. Cho, *Org. Lett.* 7 (2005) 323–326.
- [29] C. Xu, W.W. Webb, *J. Opt. Soc. Am. B.* 13 (1996) 481–491.
- [30] E. Glimsdal, M. Carlsson, B. Eliasson, B. Minaev, M. Lindgren, *J. Phys. Chem. A* 111 (2007) 244–250.
- [31] A.P. de Silva, H.Q.N. Gunaratne, T. Gunnlaugsson, A.J.M. Huxley, C.P. McCoy, J.T. Rademacher, T.E. Rice, *Chem. Rev.* 97 (1997) 1515–1566.
- [32] B. Valeur, I. Leray, *Coord. Chem. Rev.* 205 (2000) 3–40.